



Nickel(II) complexes with 2-(pyridin-3-ylmethylsulfanyl)phenylamine and halide/pseudohalides: Synthesis, structural characterisation, interaction with CT-DNA and bovine serum albumin, and antibacterial activity

Animesh Patra^a, Buddhadeb Sen^a, Sandipan Sarkar^b, Akhil Pandey^c, Ennio Zangrando^d, Pabitra Chattopadhyay^{a,*}

^a Department of Chemistry, Burdwan University, Golapbag, Burdwan 713104, India

^b Department of Applied Science and Humanities, Durgapur Institute of Advanced Technology & Management, Rajbandh, Durgapur 713212, India

^c Department of Microbiology, Midnapore College, Midnapore 721101, India

^d Dipartimento di Scienze Chimiche, Via Licio Giorgieri 1, 34127 Trieste, Italy

ARTICLE INFO

Article history:

Received 4 December 2012

Accepted 31 December 2012

Available online 9 January 2013

Keywords:

Nickel(II) complex
Crystal structure
DNA and BSA binding
Antibacterial activity

ABSTRACT

A new series of hexacoordinated octahedral nickel(II) complexes of 2-(pyridin-3-ylmethylsulfanyl)phenylamine (**L**) formulated as $[\text{Ni}(\text{L})_4(\text{X})_2]$ (**1–4**) [where $\text{X} = \text{Cl}^-$ (**1**); NCO^- (**2**); N_3^- (**3**) and NCS^- (**4**)] has been synthesised and characterised by physicochemical, spectroscopic tools. Details of structural study of complex **1** using single crystal X-ray crystallography showed that distorted tetragonal environment around nickel(II) ion has been satisfied by four pyridinic-N donors of four organic moieties (**L**) and two chloride ions. All the complexes are redox active and the electrochemical study of the complexes showed only cathodic $\text{Ni}^{\text{II}}/\text{Ni}^{\text{I}}$ redox couples in the range of -0.61 to -695 V versus Ag/AgCl. Interactions of **1** towards calf thymus-DNA by spectroscopic, viscosity-measurement and electrochemical study and towards bovine serum albumin (BSA) with the help of absorption and fluorescence spectroscopy were examined. Antibacterial activity of the complexes (**1–4**) studied by agar disc diffusion method showed the comparable inhibition activity of the nickel(II) complexes against some pathogenic bacteria namely *Escherichia coli*, *Vibrio cholerae*, *Streptococcus pneumoniae*, *Shigella* sp. and *Bacillus cereus*.

© 2013 Elsevier Ltd. All rights reserved.

1. Introduction

A considerable amount of attention is currently being shown in the synthesis of geometrically distorted nickel(II) complexes with mixed nitrogen and sulfur donor sets [1–4]. Nickel is present in the active sites of several important classes of metalloproteins, as either a homodinuclear or a heterodinuclear species. The active site of 2-mercaptoethanol-inhibited urease [5] contains two Ni centres bridged by thiolate donors, while thiolate bridging between Ni and Fe centres is present in the Ni/Fe hydrogenases [6–9]. The nickel coordination sphere in both of these metalloenzyme systems contains N and S donor atoms in unusual 5- or 6-coordinate arrangements with significant distortions from regular geometry. These distorted configurations often give rise to Ni centres with reversible Ni(II)/Ni(I) and Ni(III)/Ni(II) couples and low Ni(III)/Ni(II) redox potentials, characteristics which are crucial to the activity of the enzymes. These unusual structural and electronic features have led to increased interest in the synthesis of Ni(II) complexes with mixed N,S donating chelates as structural and spectroscopic models of the active sites.

* Corresponding author.

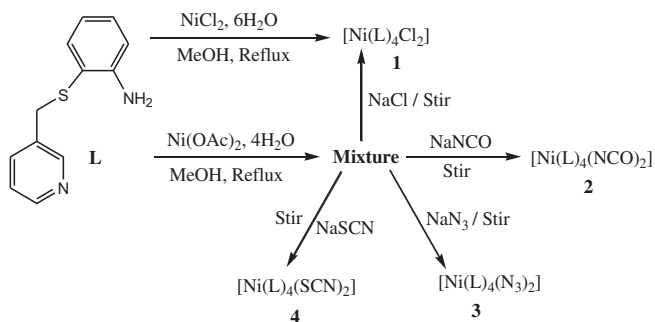
E-mail address: pabitracc@yahoo.com (P. Chattopadhyay).

As part of our continuous interest on nitrogen–sulfur polydentate chelators [10,11], here we report an account of nickel(II) complexes of 2-(pyridin-3-ylmethylsulfanyl)-phenylamine (**L**) (vide Scheme 1). Four hexacoordinated octahedral nickel(II) complexes of 2-(pyridin-3-ylmethylsulfanyl)-phenylamine (**L**) formulated as $[\text{Ni}(\text{L})_4(\text{X})_2]$ (**1–4**) [where $\text{X} = \text{Cl}^-$ (**1**); NCO^- (**2**); N_3^- (**3**) and NCS^- (**4**)] were isolated using different the nickel(II) salts used as reactant, and characterised by physicochemical and spectroscopic tools along with the detailed structural characterisations of **1** by X-ray crystallography. The DNA and protein binding study of the nickel(II) complex (**1**) has been performed spectroscopically. Antibacterial activity of complexes (**1–4**) studied by agar disc diffusion method showed the comparable inhibition activity of the nickel(II) complexes against some pathogenic bacteria namely *Escherichia coli*, *Vibrio cholerae*, *Streptococcus pneumoniae*, *Shigella* sp. and *Bacillus cereus*.

2. Experimental

2.1. Materials and physical measurements

All chemicals and reagents were obtained from commercial sources and used as received, unless otherwise stated. Solvents were distilled from an appropriate drying agent. The elemental



Scheme 1. Synthetic strategy of the complexes.

(C, H, N) analyses were performed on a Perkin Elmer model 2400 elemental analyzer. Nickel analysis was carried out by Varian atomic absorption spectrophotometer (AAS) model-AA55B, GTA using graphite furnace. Electronic absorption spectra were recorded on a JASCO UV–Vis/NIR spectrophotometer model V-570. IR spectra (KBr discs, 4000 to 300 cm^{-1}) were recorded using a Perkin-Elmer FTIR model RX1 spectrometer. The room temperature magnetic susceptibility measurements were performed by using a vibrating sample magnetometer PAR 155 model. Molar conductances (Λ_M) were measured in a systronics conductivity meter 304 model using $\sim 10^{-3}$ mol L^{-1} solutions in appropriate organic solvents. Electrochemical measurements were performed using computer-controlled CH-Instruments (Model No. – CHI620D). All measurements were carried out under nitrogen environment at 298 K with reference to SCE electrode in dimethyl sulfoxide using $[n\text{-Bu}_4\text{N}]\text{ClO}_4$ as supporting electrolyte. The fluorescence spectra of EB bound to DNA were recorded in the Fluorimeter (Hitachi-4500).

2.2. Preparation of 2-(pyridin-3-ylmethylsulfanyl)phenylamine (L)

An ethanolic solution of 3-chloromethylpyridine, hydrochloride (3.28 g, 20 mmol) was added to 2-aminobenzenethiol (2.5 g, 20 mmol) in dry ethanol containing sodium ethoxide which is prepared by dissolving sodium (1.0 g, 43.4 mmol) in dry ethanol (25 mL) under cold conditions (0–5 $^{\circ}\text{C}$). Then this mixture was allowed to stir at room temperature for 0.5 h and then it was refluxed for 3 h. The mixture was cooled to room temperature and then it was concentrated by rotary evaporation and extracted into dichloromethane (2×50 mL). The combined organic phases were washed with H_2O and then dried by anhydrous MgSO_4 , and the solvent CH_2Cl_2 was removed by rotary evaporation. The product, 2-(pyridin-3-ylmethylsulfanyl)phenylamine was obtained as a brownish yellow oil (3.1 g, 72%), which was subsequently purified by vacuum distillation for spectroscopic characterisation.

$^1\text{H NMR}$ (δ , in CDCl_3): 8.52 (s, 1H on py), 8.48 (d, 1H on py), 7.58 (d, 1H on py), 7.19 (t, 1H on py), 6.95 (m, 2H), 6.55 (m, 2H), 4.31 (broad, NH₂) and 3.99 (s, 2H). MS- EI^+ : m/e, 216 (corresponds to M^+).

2.3. Preparation of $[\text{Ni}(\text{L})_4(\text{X})_2]$ complexes (1–4)

The complexes were synthesised following a common procedure as described below. To a methanolic solution of nickel(II) acetate, tetrahydrate (249.0 mg, 1.0 mmol) was added to the solution of the organic compound (L) (864.0 mg, 4.0 mmol) in methanol (10 mL) in stirring condition at room temperature. The resulting mixture was refluxed for 3 h. To this solution aqueous solution of sodium chloride (117.0 mg, 2.0 mmol) (for **1**), sodium cyanate (130.0 mg, 2.0 mmol) (for **2**), sodium azide (130.0 mg, 2.0 mmol) (for **3**) and sodium thiocyanate (162.0 mg, 2.0 mmol) (for **4**) was

added and stirring was continued for another 1 h. The volume of the solution was reduced at room temperature by slow evaporation. The product was collected by washing with cold methanol and water; and dried. The pure crystallised product was obtained from methanol.

Complex **1** was also prepared by refluxing the mixture of 2-(pyridin-3-ylmethylsulfanyl)-phenylamine (L) (864.0 mg, 4.0 mmol) and nickel(II) chloride, hexahydrate (238.0 mg, 1.0 mmol) in methanol for 4 h. The product was collected by filtration and washing with cold methanol and water, and dried.

Complex 1: $[\text{Ni}(\text{L})_4(\text{Cl})_2]$: $\text{C}_{48}\text{H}_{48}\text{N}_8\text{S}_4\text{Ni}_1\text{Cl}_2$: Anal. Calc: C, 57.83; H, 4.74; N, 11.16; Ni, 5.82. Found: C, 57.94; H, 4.82; N, 11.26; Ni, 5.89%. IR (cm^{-1}): $\nu_{\text{C}=\text{N}}$, 1478; $\nu_{\text{C}-\text{S}}$, 752. Magnetic moment (μ , B.M.): 3.10. Conductivity (Λ_o , $\text{ohm}^{-1} \text{cm}^2 \text{mol}^{-1}$) in DMF: 44. Yield 80–85%.

Complex 2: $[\text{Ni}(\text{L})_4(\text{NCO})_2]$: $\text{C}_{50}\text{H}_{48}\text{N}_{10}\text{Ni}_1\text{S}_4\text{O}_2$: Anal. Calc: C, 59.54; H, 4.72; N, 13.82; Ni, 5.74. Found: C, 59.60; H, 4.76; N, 13.90; Ni, 5.82%. IR (cm^{-1}): $\nu_{\text{C}=\text{N}}$, 1480; $\nu_{\text{C}-\text{S}}$, 756, ν_{NCO} , 2184. Magnetic moment (μ , B.M.): 3.06. Conductivity (Λ_o , $\text{ohm}^{-1} \text{cm}^2 \text{mol}^{-1}$) in DMF: 42. Yield 75–80%.

Complex 3: $[\text{Ni}(\text{L})_4(\text{N}_3)_2]$: $\text{C}_{48} \text{H}_{48} \text{N}_{14} \text{S}_4 \text{Ni}_1$: Anal. Calc.: C, 57.26; H, 4.70; N, 19.42; Ni, 5.78. Found: C, 57.22; H, 4.76; N, 19.47; Ni, 5.82. IR (cm^{-1}): $\nu_{\text{C}=\text{N}}$, 1479; $\nu_{\text{C}-\text{S}}$, 750, ν_{N_3} , 2049. Magnetic moment (μ , B.M.): 3.08. Conductivity (Λ_o , $\text{ohm}^{-1} \text{cm}^2 \text{mol}^{-1}$) in DMF: 48. Yield 80–85%.

Complex 4: $[\text{Ni}(\text{L})_4(\text{SCN})_2]$: $\text{C}_{50}\text{H}_{48}\text{N}_{10}\text{S}_6\text{Ni}_1$: Anal. Calc: C, 57.72; H, 4.64; N, 13.41; Ni, 5.58. Found: C, 57.77; H, 4.62; N, 13.47; Ni, 5.64%. IR (cm^{-1}): $\nu_{\text{C}=\text{N}}$, 1478; $\nu_{\text{C}-\text{S}}$, 754, ν_{NCS} , 2081. Magnetic moment (μ , B.M.): 3.09. Conductivity (Λ_o , $\text{ohm}^{-1} \text{cm}^2 \text{mol}^{-1}$) in DMF: 40. Yield 75–85%.

2.4. X-ray crystal structure analysis

Crystal data and details of data collection and refinement for complex **1** was summarised in Table 1. Suitable single crystals for X-ray diffraction analysis of **1** were grown at ambient temperature by slow evaporation of a methanolic solution. Diffraction data of **1** was collected at room temperature on a Nonius DIP-1030H system, by using Mo K α radiation ($\lambda = 0.71073$ Å). Cell refinement, indexing and scaling of the data set were performed using programs DENZO and SCALEPACK [12]. The structure was solved by direct methods and subsequent Fourier analyses and refined by the full-matrix least-squares method based on F^2 with all observed reflections [13]. The contribution of hydrogen atoms at calculated positions were included in final cycles of refinement. All the calculations were performed using the WINGX System, Ver. 1.80.05 [14].

2.5. DNA binding experiments

Tris–HCl buffer (pH 7.0) solution prepared using deionised and sonicated HPLC grade water (Merck) was used in all the experiments involving CT-DNA. The CT-DNA used in the experiments was sufficiently free from protein as the ratio of UV absorbance of the solutions of DNA in tris–HCl at 260 and 280 nm (A_{260}/A_{280}) was almost ≈ 1.9 [15]. The concentration of DNA was determined with the help of the extinction coefficient of DNA solution [16]. Absorption spectral titration experiment was performed by keeping constant the concentration of the nickel(II) complex and varying the CT-DNA concentration.

In the ethidium bromide (EB) fluorescence displacement experiment, 5 μL of the EB tris–HCl solution (1.0 mmol L^{-1}) was added to 1.0 mL of DNA solution (at saturated binding levels) [17], stored in the dark for 2.0 h. Then the solution of the nickel(II) complex was titrated into the DNA/EB mixture and diluted in tris–HCl buffer to 5.0 mL to get the solution with the appropriate Ni(II) complex/CT-DNA mole ratio. Before measurements, the mixture was shaken up

Table 1
Crystal data and details of refinement data for complex **1**.

Complex 1	
Empirical formula	C ₁₈ H ₁₈ Cl ₂ N ₈ NiS ₄
Formula weight	994.79
Crystal system	tetragonal
Space group	I4
<i>a</i> (Å)	13.924(3)
<i>b</i> (Å)	13.924(3)
<i>c</i> (Å)	12.523(3)
α (°)	90.00
β (°)	90.00
γ (°)	90.00
Volume (Å ³)	2427.9(9)
<i>Z</i>	2
ρ_{calc} (g/cm ³)	1.640
<i>F</i> (000)	1036
θ Range (°)	2.19–29.60
μ (Mo K α) (mm ⁻¹)	0.724
Independent reflections	14493
Temperature (K)	293(2)
Observed data [<i>I</i> > 2.0 σ (<i>I</i>)]	2892
<i>R</i> ₁	0.0370, 0.0518
<i>wR</i> ₂	0.0983, 0.1074
Goodness-of-fit (GOF)	0.948

and incubated at room temperature for 30 min. The fluorescence spectra of EB bound to DNA were obtained at an emission wavelength of 522 nm in the Fluorimeter (Hitachi-4500).

To adjudge the binding mode (groove/intercalative) of **1** with DNA, the well known method using Ostwald's viscometer was used. Titrations were performed by introducing nickel(II) complex (**1**) (0.5–3.5 μM) into a CT-DNA solution (5.0 μM) present in the viscometer. From the observed flow time of CT-DNA-containing solution corrected from the flow time of buffer alone (t_0), $\eta = t - t_0$, the calculated viscosity values of the solutions were used for plotting the $(\eta/\eta_0)^{1/3}$ versus the ratio of the concentration of **1** and CT-DNA, where η is the viscosity of CT-DNA in the presence of the compound and η_0 is the viscosity of CT-DNA alone.

2.6. Protein (bovine serum albumin) binding experiments

The sample was placed in quartz cuvettes of 1 cm optical path. In these experiments, 3 mL of BSA solution were poured into the cell. The samples were carefully degassed using pure nitrogen gas for 15 min. Emission spectra were recorded after addition of the appropriate concentration of the nickel(II) complexes in the same buffer. The samples were excited at 280 nm.

2.7. In vitro antibacterial assay

The biological activities of synthesised ligand (**L**) and its nickel(II) complexes have been studied for their antibacterial activities by agar well diffusion method [18–21]. The antibacterial activities were done at 100 $\mu\text{g}/\text{mL}$ concentrations of different compounds in DMF solvent by using four pathogenic gram negative bacteria (*E. coli*, *V. cholerae*, *S. pneumoniae*, *Shigella* sp.) and one gram positive pathogenic bacteria (*B. cereus*). Stock cultures of the test bacterial species were maintained on Nutrient Agar media by sub culturing in slants. The media were prepared by adding beef extract 3 g, peptone 5 g, agar 15 g, distilled water 1000 mL and the pH was adjusted at 7.2. Media was sterilised in the autoclave at 15 lb pressure for 20 min. 20 mL of media was poured in each Petri dish and allowed to solidify. After solidification, nutrient agar plates were swabbed by sterile cotton swabs with 12 h old 0.1 mL broth culture of respective bacteria. The wells were bored with cork-borer and the agar plugs were removed. Then solution of ligand and its nickel(II) complexes were added to the agar wells. DMF was used as a negative control. The Petri dishes were incu-

bated at 37 °C for 24 h. After incubation plates were observed for the growth of inhibition zones. The diameter of the zone of inhibition was measured in millimeters.

3. Results and discussion

3.1. Synthesis and characterisation

The organic compound, 2-(pyridin-3-ylmethylsulfanyl)-phenylamine (**L**) was synthesised by the reaction of 2-aminothiophenol and 3-chloromethylpyridine in presence of sodium ethoxide. The product obtained by this procedure even before distillation is of a high purity enough for the subsequent synthetic steps. The identity and purity were verified using spectroscopic tools. The complexes (**1–4**) were obtained in good yield from the reaction of the nickel(II) acetate, tetrahydrate with four equimolar amount of organic moiety in the methanol medium followed by the addition of respective aqueous solution of chloride/pseudohalides to the reaction mixture. Complex **1** can also be prepared directly by refluxing the mixed solution of nickel(II) chloride and **L** in 1:4 mol ratio.

In these complexes (**1–4**), the ligand (**L**) acts as a monodentate neutral N donor ligand since only the pyridinic-N atom coordinates with central nickel(II) ion keeping amine and sulfur atom uncoordinated, though **L** has three donor (NNS) centres. All the complexes are soluble in common organic solvents and are polymeric in nature through H-bonding. Conductivity measurement of the complexes in dimethyl sulfoxide showed conductance values in range of 40–48 (Λ_{m} , $\text{ohm}^{-1} \text{cm}^2 \text{mol}^{-1}$) which suggests that all complexes are non-electrolytes. The magnetic moments (μ) at room temperature of these complexes are 3.10, 3.06, 3.08 and 3.09 which indicate all complexes are high spin distorted octahedral geometry.

3.2. Structure of complex **1**

The crystal structure of $[\text{Ni}(\text{L})_4\text{Cl}_2]$ is shown in Fig. 1 together with the atomic labelling scheme for all of the atoms except the hydrogens. The crystallographic data and details of the structure determinations are given in Table 1 while selected bond lengths and bond angles appear in Table 2.

The complex **1** exists as an octahedral mononuclear structure. Here, the nickel(II) ion is located on a fourfold axis with a symmetry plane and exist as a distorted tetragonal environment with ligand **L** and two *trans* chloride anions. The ligand **L** only acts as a monodentate fashion through the pyridine nitrogen atom, while the amine group remains uncoordinated like a tail. In the equatorial plane, each nickel(II) ion is coordinated by four pyridinic nitrogen atoms and two chloride anions in axial of the octahedron in which the bond lengths of Ni(II)–N(1), Ni(II)–Cl(1) and Ni(II)–Cl(2) are (2.13), (2.44) and (2.45) Å, respectively. This bond length also indicates that the high electron density of four pyridinic-N atom form strong bond with nickel-atom but two *trans* Cl⁻ atom have comparatively lower electron density form weak bond with nickel-atom and two Ni–Cl distances are comparable. It is noted that the uncoordinated amine groups are connected as a 2D layer structure through intermolecular N–H...N–H hydrogen bonding interactions (Fig. 2), in which the bond distance of N–N is (3.12 Å).

Crystal packing of the complex **1** shows a polynuclear arrangement through the interaction between chloride atom and amino groups (Fig. 3), down axis showing N(2)–Cl(1) distances are of 3.64 Å.

3.3. Spectral studies

The infrared spectral data of all the complexes exhibit characteristic strong to medium intensity band in the region of 1468–

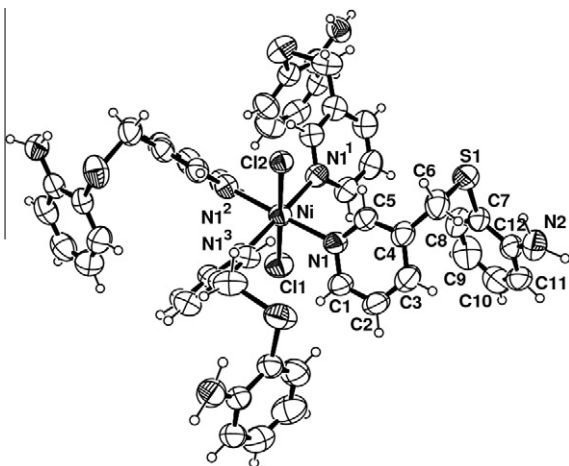


Fig. 1. An ORTEP diagram of Ni complex **1** located on a fourfold axis.

Table 2
Selected bond distances (Å) and bond angles (°) for **1**.

Bond lengths (Å)		Bond angles (°)	
Ni–N(1)	2.135(2)	N(1)–Ni–N(1)	89.979(3)
Ni–Cl(1)	2.4412(17)	N(1)–Ni–N(1)	177.82(13)
Ni–Cl(2)	2.4593(14)	N(1)–Ni–Cl(1)	90.09(7)
		N(1)–Ni–Cl(2)	88.91(7)
		Cl(1)–Ni–Cl(2)	180.0

1472 and 758–761 cm^{-1} , which are assigned to $\nu_{\text{C}=\text{N}}$ stretching and $\nu_{\text{C}-\text{S}}$, respectively. A broad band around at 3421 cm^{-1} attributable to amide group and an intense band centred at 2184 cm^{-1} assignable to ν_{NCO} (**2a**), 2049 cm^{-1} assignable to ν_{N_3} (**2b**) and an intense band centred at 2084 cm^{-1} assignable to ν_{NCS} (**2c**). The observations support the presence of the ligand frame coordinated to nickel(II) centre through pyridinic-N and uncoordinated thioether-S as $\nu_{\text{C}-\text{S}}$ was observed in the range of 780–790 cm^{-1} which was generally observed in free ligand [11].

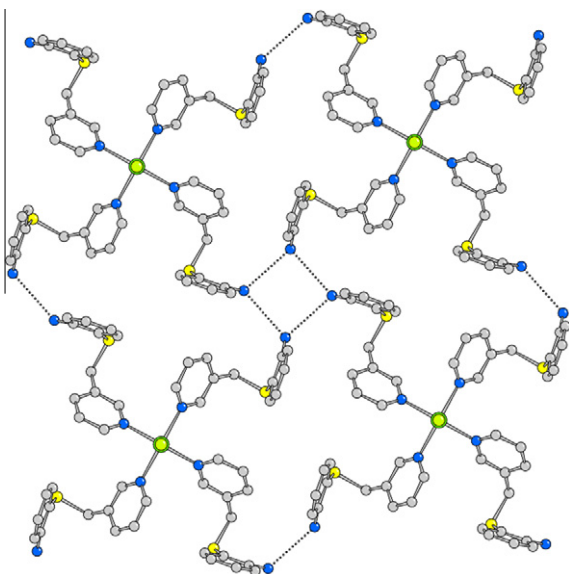


Fig. 2. Packing of complex **1** down axis *c* showing the H-bonding scheme involving the amino groups (N–N distance 3.12 Å). These connections lead to 2D layered structure.

The electronic absorption spectra of the complexes **1** and **2–4** were recorded at room temperature using DMF as solvent and the data are tabulated in Table 3. Each complex shows an absorption ranging from 350 to 450 nm, which was not observed for the corresponding free ligand. It suggests that the absorption bands of all complexes are assignable to the LMCT transition from the pyridinic-N of organic moiety to the Nickel centre. All the spectra of complexes lower than 400 nm are due to intramolecular $\pi \rightarrow \pi^*$ and $n \rightarrow \pi^*$ transitions for the aromatic ring. In octahedral nickel(II) complexes, three spin allowed transitions are expected from the energy level diagram for d^8 ions due to ${}^3A_{2g} \rightarrow {}^3T_{1g}(\text{P})$, ${}^3A_{2g} \rightarrow {}^3T_{1g}(\text{F})$, ${}^3A_{2g} \rightarrow {}^3T_{2g}$ transitions, which are observed at low to high wavelengths, respectively. The bands at 424 and 687 nm, which may be assigned to ${}^3A_{2g} \rightarrow {}^3T_{1g}(\text{P})$ and ${}^3A_{2g} \rightarrow {}^3T_{1g}(\text{F})$ transition, respectively. Again the intensity of the peak at around 850 nm observed due to the ${}^3A_{2g} \rightarrow {}^3T_{2g}$ transition. These observations suggest an octahedral geometry of the nickel(II) ion.

3.4. Electrochemistry

The electrochemical properties of the complexes (**1–4**) were examined by cyclic voltammeter using a Pt-disk working electrode and a Pt-wire auxiliary electrode in dry dimethylformamide using 0.1 M [*n*-Bu₄N]ClO₄ as the supporting electrolyte. The voltammetric parameters were studied in the scan rate interval 50–400 mV s^{-1} . From the voltammetric data given in Table 3, it was observed that a quasi-reversible voltammogram corresponding to $\text{Ni}^{\text{II}}/\text{Ni}^{\text{I}}$ redox couples was obtained in every cyclic voltammogram of the $[\text{Ni}(\text{L})\text{X}_2]$. The $E_{1/2}$ values for this $\text{Ni}^{\text{II}}/\text{Ni}^{\text{I}}$ redox couples were in the range of -0.61 to -0.695 V versus Ag/AgCl and the ratio between the cathodic peak current and the square root of the scan rate is approximately constant. The fact of the highest ΔE value (200 mV) for complex **1** and the lowest ΔE value (170 mV) for complex **4** indicates that the $[\text{Ni}^{\text{I}}(\text{L})_4\text{Cl}_2]$ state is comparatively more stable than the $[\text{Ni}^{\text{I}}(\text{L})_4(\text{NCS})_2]$. This is due to the fact of the existence of the coligand (chloride/cyanate/azide/isothiocyanate) with **L** in the coordination sphere of the complexes (**1–4**) and the ΔE values (170–200 mV) are in the accordance with the hardness of the coligands. Eventually, the presence of comparatively hard isothiocyanate donor ligand in complex **4** like to return to the $[\text{Ni}^{\text{II}}(\text{L})_4(\text{N}_3)_2]$ state from its corresponding $[\text{Ni}^{\text{I}}(\text{L})_4(\text{N}_3)_2]$ state as usual. The peak potential shows a small dependence on the scan rate. The ratio i_{pc} to i_{pa} is close to unity. From these data, it can be deduced that the redox couple is related to a quasi-reversible one-electron transfer process controlled by diffusion.

3.5. DNA-binding studies

The binding interaction of the nickel(II) complex **1** with calf thymus DNA (CT-DNA) has been investigated with the help of spectroscopic, viscosity-measurements and electrochemical study. This study showed that the complex **1** interact with CT-DNA in groove binding mode of interaction. As a result, this study was performed taking only complex **1** which is structurally very close to complexes **2–4**.

3.5.1. Spectrophotometric study

Electronic absorption spectroscopy is an effective method to examine the binding modes of metal complexes with DNA. In general, binding of the nickel(II) complex to the CT-DNA helix is examined by an increase of the absorption band (c.a. 264 nm) of nickel(II) complex. This trend of increase of absorbance indicates that there is the involvement of strong interactions between complex and the base pairs of DNA [22]. The absorption spectra of the nickel(II) complex **1** in the absence and presence of CT-DNA are given in (Fig. 4). The extent of the hyperchromism in the charge

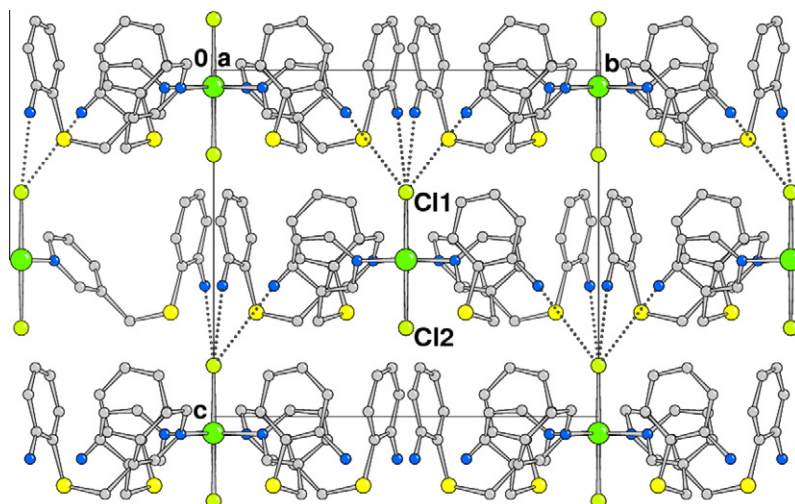


Fig. 3. Packing of complex **1** down axis *a* showing the interaction between Cl1 and amine groups NH₂.

Table 3
UV–Vis spectral and electrochemical data.

Compound	λ , nm (ϵ , dm ³ mol ⁻¹ cm ⁻¹) ^a	Electrochemical data ^{a,b}			
		E_{pa} (V)	E_{pc} (V)	$E_{1/2}$, V (ΔE , mV)	i_{pc}/i_{pa}
1	234(22258), 265(2853), 307(139), 422(100)	-0.51	-0.71	-0.61 (200)	1.07
2	263(11654), 309(7097), 422(951), 686(366)	-0.57	-0.75	-0.66 (180)	1.02
3	263(10172), 310(6539), 424(435), 687(172)	-0.54	-0.73	-0.635 (190)	1.05
4	264(16388), 310(10388), 422(1284), 686(431)	-0.61	-0.78	-0.695 (170)	1.01

^a In DMF.

^b Scan rate of 100 mV s⁻¹.

transfer band is generally consistent with the strength of interaction [23–25]. In order to further illustrate the binding strength of the nickel(II) complex with CT-DNA, the intrinsic binding constant K_b was determined from the spectral titration data using the following equation [26]:

$$[\text{DNA}]/(\epsilon_a - \epsilon_f) = [\text{DNA}]/(\epsilon_a - \epsilon_f) + 1/[K_b(\epsilon_a - \epsilon_f)]$$

where [DNA] is the concentration of DNA, ϵ_f , ϵ_a and ϵ_b correspond to the extinction coefficient, respectively, for the free nickel(II) complex, for each addition of DNA to the nickel(II) complex and for the nickel(II) complex in the fully bound form. From the [DNA]/($\epsilon_a - \epsilon_f$) versus [DNA] plot (Fig. 5), the binding constant K_b for the nickel(II) complex **1** was estimated to be $1.65 \times 10^5 \text{ M}^{-1}$ ($R = 0.99135$ for four points) indicating in terms of groove binding [27].

3.5.2. Spectrofluorimetric study

Fluorescence intensity of EB bound to CT-DNA at excitation wavelength of 522 nm shows a decreasing trend with the increasing concentration of the complex **1** (Fig. 6). The quenching of EB bound to DNA by the complex **1** is in agreement with the linear Stern–Volmer equation [28]

$$I_0/I = 1 + K_{sv}[Q]$$

where, I_0 and I represent the fluorescence intensities in absence and presence of quencher, respectively. K_{sv} is a linear Stern–Volmer quenching constant, Q is the concentration of quencher. The K_{sv} value calculated from the plot (Fig. 7) of I_0/I versus [complex] for the complex **1** is 3.12×10^4 ($R = 0.99529$ for four points), suggesting a strong affinity of the complex **1** to CT-DNA.

Number of binding sites can be calculated from fluorescence titration data using the following equation [29]

$$\log[(I_0 - I)/I] = \log K + n \log [Q]$$

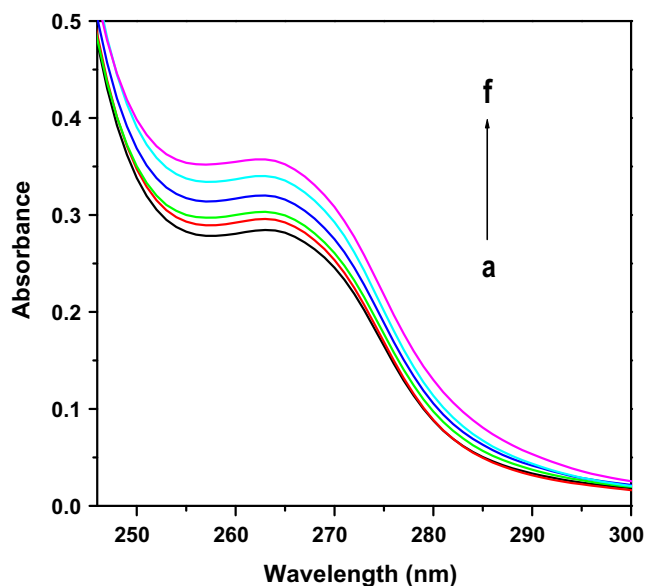


Fig. 4. Electronic spectral titration of complex **1** with CT-DNA at 266 nm in tris-HCl buffer. Arrow indicates the direction of change upon the increase of DNA concentration.

K and n is the binding constant and binding site of complex **1** to CT-DNA, respectively. The number of binding sites (n) determined from the intercept of $\log[(I_0 - I)/I]$ versus $\log [Q]$ is 0.92 which indicates less association of the complex **1** to the number of DNA bases, also suggesting strong affinity of the complex **1** through surface or groove binding.

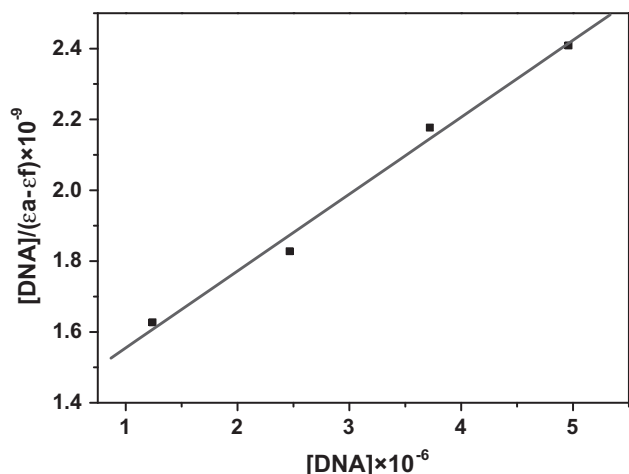


Fig. 5. Plot of $[DNA]/(\epsilon_a - \epsilon_f) \times 10^{-9}$ vs. $[DNA] \times 10^{-6}$ for the absorption titration of CT-DNA with the nickel (II) complex **1** in Tris-HCl buffer.

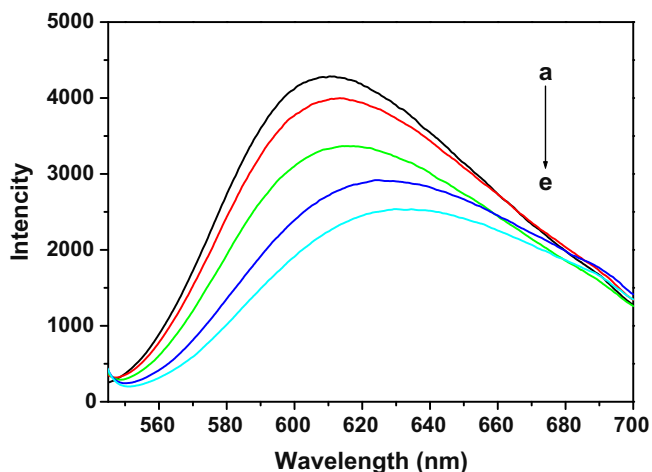


Fig. 6. Emission spectra of the CT-DNA-EB system in tris-HCl buffer upon the titration of the complex **1**. $\lambda_{ex} = 522$ nm. Arrow shows the intensity change upon the increase of the complex concentration.

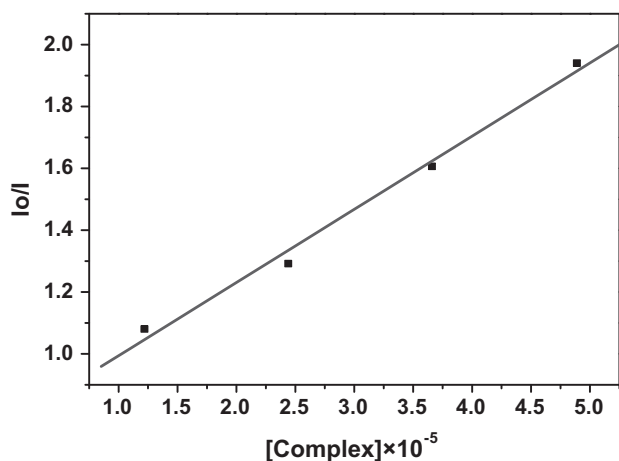


Fig. 7. Plot of I_0/I vs. $[Complex] \times 10^{-5}$ for the titration of nickel (II) complex **1** with CT-DNA-EB system in tris-HCl buffer.

3.5.3. Viscosity technique

From the experiment on the viscosity measurements study, it was observed that there is almost no effect on the relative viscosity

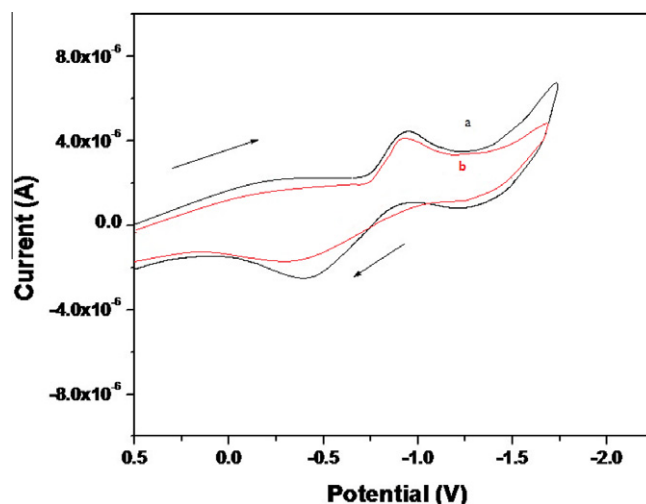


Fig. 8. Cyclic voltammograms of complex **1** in tris-HCl buffer in the absence (a) and presence (b) of CT-DNA. $\nu = 1 \text{ V s}^{-1}$.

of the DNA solution by adding the complex. This study suggests that the binding mode is groove binding which is in support of the above results obtained in spectroscopic study. otherwise if it be intercalative candidate, then the change of the relative viscosity of the DNA solution was observed because intercalation leads to an increase in the DNA viscosity by lengthening the DNA helix, or the non-classical intercalation could bend (or kink) the DNA helix and reduce its effective length and, concomitantly, its viscosity [30,31].

3.5.4. Electrochemical study

Electrochemical investigations is useful technique to analyse metal-DNA interactions over spectroscopic methods [32,33]. The binding nature of the nickel(II) complex **1** with DNA, has been shown in Fig. 8. Cyclic voltammograms of the nickel(II) complex **1** in the absence and presence of CT-DNA is exhibited significant shifts in the anodic and cathodic peak potentials followed by decrease in both peak currents, indicating the interaction existing between the nickel(II) complex and CT-DNA. Equilibrium binding constants K_R/K_O can be calculated by using the shift value of the formal potential (ΔE^0) of Ni(II)/Ni(I) according to the following equation [34]:

$$\Delta E^0 = E_b^0 - E_f^0 = 0.0591 \log(K_R/K_O)$$

where E_b^0 and E_f^0 are the formal potentials of the bound and free complex forms, respectively, and K_R and K_O are the corresponding binding constants for the binding of reduction and oxidation species to DNA, respectively. Ratio of equilibrium binding constants, K_R/K_O is calculated to be 2.17 which indicate the binding of DNA with the reduced form of the complex **1** over its oxidised form.

3.6. Protein (bovine serum albumin) binding experiments

3.6.1. Absorption characteristics of BSA-nickel(II) complex **1**

The absorption spectra of BSA in the absence and presence of Ni(II) complex **1** (other complexes give same binding interaction) were studied at different concentrations (Fig. 9). From this study we observed that absorption of BSA increases regularly upon increasing the concentration of the complex. It is may be due to the adsorption of BSA on the surface of the complex. From these data the apparent association constant (K_{app}) determined of the complexes with BSA has been determined using the following equation [27]:

$$1/(A_{obs} - A_0) = 1/(A_c - A_0) + 1/K_{app}(A_c - A_0)[comp]$$

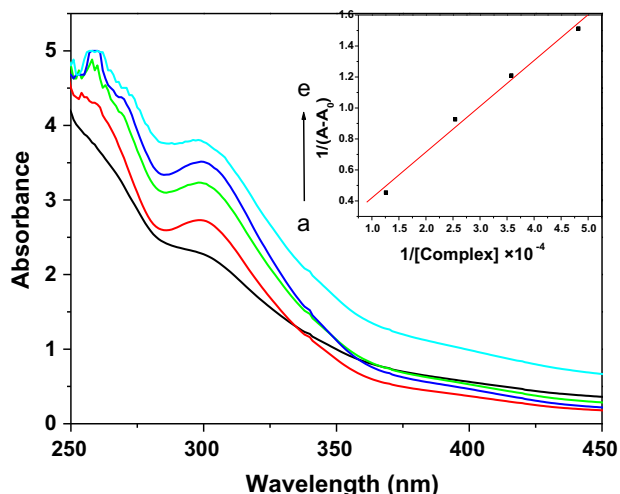


Fig. 9. Electronic spectral titration of complex **1** with BSA at 266 nm in tris-HCl buffer. Arrow indicates the direction of change upon the increase of BSA concentration.

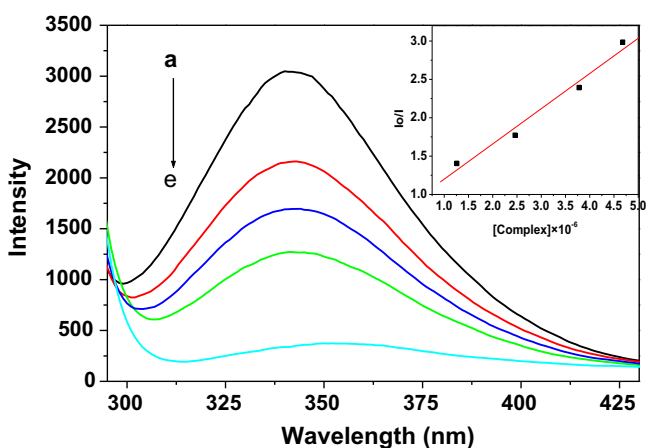


Fig. 10. Fluorescence quenching of BSA in the presence of various concentrations of the complex **1**, $[\text{complex}] = 0, 1, 2, 3$ and $4 \times 6.35 \times 10^{-6}$ M.

where, A_{obs} is the observed absorbance of the solution containing different concentrations of the complex at 280 nm, A_0 and A_c are the absorbances of BSA and the complex at 280 nm, respectively, with a concentration of complex and K_{app} represents the apparent association constant. The enhancement of absorbance at 280 nm was due to absorption of the surface complex, based on the linear relationship between $1/(A_{\text{obs}} - A_0)$ versus reciprocal concentration of the complex with a slope equal to $1/K_{\text{app}}(A_c - A_0)$ and an intercept equal to $1/(A_c - A_0)$ (inset Fig. 9). The value of the apparent association constant (K_{app}) determined from this plot is $2.37 \times 10^4 \text{ M}^{-1}$ ($R = 0.99459$ for four points).

3.6.2. Fluorescence quenching of BSA by complex **1**

The fluorescence emission spectrum of BSA were studied with increasing the concentration of the complex and represented in Fig. 10. With the addition of complex BSA fluorescence emission is quenched. The fluorescence quenching is described by the Stern–Volmer relation [28] described above. A linear plot (inset, Fig. 10) between I_0/I against $[\text{complex}]$ was obtained and from the slope we calculated the K_{SV} as 4.51×10^4 ($R = 0.99275$ for four points).

3.7. Antibacterial activity

Antibacterial activity of the ligand and corresponding complexes are recorded in Table S1. From the antibacterial studies it is inferred that all the complexes have higher activity than the organic moiety (**L**). The increased activity of the metal chelates can be explained based on the oxidation state of the metal ion, overtone concept and the Tweedy chelation theory. It is observed that, in a complex, the positive charge of the metal is partially shared with the donor atoms present in the ligands, further it increases the delocalisation of π -electrons over the whole chelate ring and lipophilic character of the metal complexes also increases. This increased lipophilicity enhances the penetration of complexes into the lipid layer of the bacterial cell membranes and blocks the metal binding sites in enzymes of microorganisms. These complexes also disturb the respiration process of the cell and thus block the synthesis of proteins, which restricts further growth of the microorganisms. The complex **1** act as a higher activity than ligand and other complexes due to higher lipophilicity.

4. Conclusion

Four new mononuclear nickel(II) complexes with a new organic moiety, 2-(pyridin-3-ylmethylsulfanyl)phenylamine (**L**) and halide/pseudohalides (**1–4**) have been synthesised and characterised by spectroscopic and electrochemical techniques along with the detailed structural characterisation of complex **1** by single crystal X-ray diffraction. Here, **L** behaves as a monodentate ligand though it has tridentate NNS donor centres. The crystallographic analysis of **1** indicates that the nickel(II) ion is in octahedral geometry with two chloride ions occupying *trans* position and four pyridinic-N of the ligand, **L**. Abundant intermolecular N–H...N–H hydrogen bonding the complex **1** connected as a 2D layer framework and shows polynuclear arrangement through the interaction between chloride atom and amine groups. The electrochemical study of the complexes showed a quasi-reversible one-electron transfer process for cathodic $\text{Ni}^{\text{II}}/\text{Ni}^{\text{I}}$ redox couples in the range of -0.61 to -695 V versus Ag/AgCl. The spectroscopic study of interaction of **1** with CT-DNA showed the groove binding mode of complex **1** and it is also in accordance with the unchanged values of the viscosity of the DNA solution upon addition of complex **1**. The absorption as well as fluorescence spectroscopy tools are used to study these interactions, proving the formation of a ground state BSA– $[\text{Ni}(\text{L})_4\text{Cl}_2]$ complex. From the antibacterial studies it could be inferred that metal complexes have higher activity than ligand due to chelation. All four nickel(II) complexes have higher antibacterial activity than ligand **L** against five pathogenic bacteria (*E. coli*, *V. cholerae*, *S. pneumonia*, *Shigella* sp. and *B. cereus*).

Acknowledgements

Financial supports from Department of Science and Technology (DST), New Delhi and Council of Scientific and Industrial Research (CSIR), New Delhi, India are gratefully acknowledged. E. Zangrando thanks MIUR-Rome, PRIN 2007HMTJWP_002 for financial support.

Appendix A. Supplementary material

CCDC 885271 contains the supplementary crystallographic data for complex **1**. These data can be obtained free of charge via <http://www.ccdc.cam.ac.uk/conts/retrieving.html>, or from the Cambridge Crystallographic Data Centre, 12 Union Road, Cambridge CB2 1EZ, UK; fax: (+44) 1223-336-033; or e-mail: deposit@ccdc.cam.ac.uk. Supplementary data associated with this article can be found, in the online version, at <http://dx.doi.org/10.1016/j.poly.2012.12.031>.

References

- [1] H. Frydendahl, H. Toftlund, Jan. Becher, J.C. Dutton, K.S. Murray, L.F. Taylor, O.P. Anderson, E.R.T. Tiekink, *Inorg. Chem.* 34 (1995) 4467.
- [2] R.K. Henderson, E. Bouwman, A.L. Spek, J. Reedijk, *Inorg. Chem.* 36 (1997) 4616.
- [3] B. Adhikari, O.P. Anderson, R. Hazell, S.M. Miller, C.E. Olsen, H. Toftlund, *Dalton Trans.* (1997) 4539.
- [4] F. Lions, K.V. Martin, *J. Chem. Soc.* (1957) 127.
- [5] S. Wang, M.H. Lee, R.P. Hausinger, P.A. Clark, D.E. Wilcox, R.A. Scott, *Inorg. Chem.* 33 (1994) 1589.
- [6] R.P. Happe, W. Roseboom, A.J. Pierik, S.P. Albracht, K.A. Bagley, *Nature* 385 (1997). 126–126.
- [7] M.W.W. Adams, *Biochim. Biophys. Acta* 1020 (1990) 115.
- [8] A.E. Przybyla, J. Robins, N. Menon, H.D. Peck, *J. FEMS Microbiol. Rev.* 88 (1992) 109.
- [9] K.L. Kovacs, L.C. Seefeldt, G. Tigyi, C.M. Doyle, L.E. Mortenson, D.J. Arp, *J. Bacteriol.* 171 (1989) 430.
- [10] S. Sarkar, S. Sen, S. Dey, E. Zangrando, P. Chattopadhyay, *Polyhedron* 29 (2010) 3157. and references therein.
- [11] A. Patra, S. Sarkar, M.G.B. Drew, E. Zangrando, P. Chattopadhyay, *Polyhedron* 28 (2009) 1261.
- [12] C. Ganesamoorthy, M.S. Balakrishna, P.P. George, J.T. Mague, *Inorg. Chem.* 46 (2007) 848.
- [13] G.M. Sheldrick, *SHELX97 Programs for Crystal Structure Analysis* (Release 97-2), University of Göttingen, Germany, 1998.
- [14] L.J.J. Farrugia, *Appl. Crystallogr.* 32 (1999) 837.
- [15] E. Bouwman, A. Burik, J.C.T. Hove, W.L. Driessen, J. Reedijk, *Inorg. Chim. Acta* 150 (1988) 125.
- [16] E. Bouwman, R. Day, W.L. Driessen, W. Tremel, B. Krebs, J.S. Wood, J. Reedijk, *Inorg. Chem.* 27 (1988) 4614.
- [17] W.G. Haanstra, W.L. Driessen, R.A.G. de Graaff, J. Reedijk, Y.F. Wang, C.H. Stam, *Inorg. Chim. Acta* 186 (1991) 215.
- [18] E.H. Cordes, W.P. Jencks, *J. Am. Chem. Soc.* 84 (1962) 832.
- [19] C.E. Clifton, G. Morrow, *J. Bacteriol.* 31 (1936) 441.
- [20] C. Sheikh, M.S. Hossain, M.S. Easmin, M.S. Islam, M. Rashid, *Biol. Pharma. Bull.* 27 (2004) 710.
- [21] S. Shivhare, D.G. Mangla, *J. Curr. Pharm. Res.* 6 (2011) 16.
- [22] A. Ambroise, B.G. Maiya, *Inorg. Chem.* 39 (2000) 4264.
- [23] S.A. Tysoe, R.J. Morgan, A.D. Baker, T.C. Streckas, *J. Phys. Chem.* 97 (1993) 2172.
- [24] J.K. Barton, A.T. Danishefsky, J. Goldberg, *J. Am. Chem. Soc.* 106 (1984) 2172.
- [25] J.M. Kelly, A.B. Tossi, D.J. McConnell, C. OhUigin, *Nucleic Acids Res.* 13 (1985) 6017.
- [26] R. Vijayalakshmi, M. Kanthimathi, V. Subramanian, B.U. Nair, *Biochim. Biophys. Acta* 1475 (2000) 157.
- [27] A.M. Pyle, J.P. Rehmann, R. Meshoyrer, C.V. Kumar, N.J. Turro, J.K. Barton, *J. Am. Chem. Soc.* 111 (1989) 3051.
- [28] O. Stern, M. Volmer, *Zeitschr. Phys.* 20 (1919) 183.
- [29] A. Kathiravan, R. Renganathan, *Polyhedron* 28 (2009) 1374.
- [30] S. Satyanarayana, J.C. Dabrowiak, J.B. Chaires, *Biochemistry* 31 (1992) 9319.
- [31] S. Satyanarayana, J.C. Dabrowiak, J.B. Chaires, *Biochemistry* 32 (1993) 2573.
- [32] S. Mahadevan, M. Palaniandavar, *Inorg. Chem.* 37 (1998) 693.
- [33] M.T. Carter, M. Rodriguez, A.J. Bard, *J. Am. Chem. Soc.* 111 (1989) 8901.
- [34] M.T. Carter, A.J. Bard, *J. Am. Chem. Soc.* 109 (1987) 7528.